Biogeosciences Discuss., 11, 16911–16951, 2014
www.biogeosciences-discuss.net/11/16911/2014/
doi:10.5194/bgd-11-16911-2014

Biogeosciences Discussions
Open Access

On the use of the post-closure method uncertainty band to evaluate the performance of land surface models against eddy covariance flux data

J. Ingwersen[1], K. Imukova[1], P. Högy[2], and T. Streck[1]

[1]Institute of Soil Science and Land Evaluation, Universität Hohenheim, 70593 Stuttgart, Germany
[2]Institute of Landscape and Plant Ecology, Universität Hohenheim, 70593 Stuttgart, Germany

Received: 27 October 2014 – Accepted: 31 October 2014 – Published: 9 December 2014

Correspondence to: J. Ingwersen (joachim.ingwersen@uni-hohenheim.de)

Published by Copernicus Publications on behalf of the European Geosciences Union.

Abstract

The energy balance of eddy covariance (EC) flux data is normally not closed. Therefore, at least if used for modeling, EC flux data are usually post-closed, i.e. the measured turbulent fluxes are adjusted so as to close the energy balance. At the current state of knowledge, however, it is not clear how to partition the missing energy in the right way. Eddy flux data therefore contain some uncertainty due to the unknown nature of the energy balance gap, which should be considered in model evaluation and the interpretation of simulation results. We propose to construct the post-closure method uncertainty band (PUB), which essentially designates the differences between non-adjusted flux data and flux data adjusted with the three post-closure methods (Bowen ratio, latent heat flux (LE) and sensible heat flux (H) method). To demonstrate this approach, simulations with the NOAH-MP land surface model were evaluated based on EC measurements conducted at a winter wheat stand in Southwest Germany in 2011, and the performance of the Jarvis and Ball–Berry stomatal resistance scheme was compared. The width of the PUB of the LE was up to $110\,\mathrm{W\,m^{-2}}$ (21 % of net radiation). Our study shows that it is crucial to account for the uncertainty of EC flux data originating from lacking energy balance closure. Working with only a single post-closing method might result in severe misinterpretations in model-data comparisons.

1 Introduction

The eddy covariance (EC) technique is used worldwide to measure surface energy and matter fluxes. Until the 1980s, its application was restricted to a small circle of micrometeorologists. The equipment was expensive, its operation needed many years of experience, and data processing was complex and computationally demanding. During the last three decades, however, the installation and operation of EC flux stations has increasingly become "plug-and-play", and the development of software packages such as TK3 (Mauder and Foken, 2011) or EddyPro (LI-COR Inc., 2012)

BGD
11, 16911–16951, 2014

allow non-micrometeorologists to process and evaluate EC data. This has led to a widespread use of the EC technique. Nowadays, the method is used by a broad community of scientists. It is applied by meteorologists, agronomists, biologists, hydrologists, forest and environmental scientists, geographers etc. An impressive example of its worldwide use is the global trace gas flux network FLUXNET, which consists today of more than 400 EC stations dispersed across most of the world's climatic zones and biomes (Baldocchi et al., 2012).

The EC method is based on the assumption that the transport of energy and matter close to the land surface within the boundary layer is fully turbulent. Under (quasi-) stationary conditions, with a homogeneous surface and some less important assumptions, the sensible heat flux (H, $\mathrm{W\,m^{-2}}$) and the latent heat flux (λE, $\mathrm{W\,m^{-2}}$) can be determined by measuring the covariance of the scalar variable of interest and the vertical wind speed (w, $\mathrm{m\,s^{-1}}$) according to Eqs. (1) and (2) as follows:

$$H = \rho C_p \overline{\theta' w'} \tag{1}$$

$$\lambda E = \rho \overline{q' w'} \tag{2}$$

For H, the scalar of interest is the potential temperature (θ, K). In the case of λE, it is the specific humidity of air (q, $\mathrm{kg\,kg^{-1}}$). The symbol ρ denotes air density ($\mathrm{kg\,m^{-3}}$), assumed constant, and C_p is the heat capacity of air ($\mathrm{J\,kg^{-1}\,K^{-1}}$). Besides measuring these turbulent fluxes, EC stations are usually equipped with a net radiometer (R_N, $\mathrm{W\,m^{-2}}$) and devices for measuring the soil heat flux (G, $\mathrm{W\,m^{-2}}$). These two measurements are used to evaluate the energy balance closure (EBC) of the EC flux data. Under ideal conditions:

$$R_\mathrm{N} - G = \lambda E + H \tag{3}$$

The left-hand side of Eq. (3) is termed the available energy, and the right term is the sum of the turbulent fluxes. With measured data, however, this equation is rarely

BGD
11, 16911–16951, 2014

fulfilled. Typically, the sum of the measured turbulent fluxes is lower than the measured available energy. The degree of EBC is often expressed as the energy balance ratio (EBR):

$$\mathrm{EBR} = \frac{\lambda E + H}{R_\mathrm{N} - G} \tag{4}$$

The energy imbalance is typically in the range of 10–30 % of the available energy (Wilson et al., 2002; Twine et al., 2000). This means that, in terms of energy flux, on a sunny summer day the imbalance can reach values of up to 150 $\mathrm{W\,m^{-2}}$ over a crop stand. Possible reasons discussed for the imbalance in the literature (e.g., Foken, 2008; Twine et al., 2000) can be assigned to two types: (I) measurement errors, and (II) errors due to invalid assumptions. There is growing evidence that measuring errors cannot fully explain the systematic energy gap of the EC flux data (Foken, 2008). Type II errors include unconsidered energy storage terms or neglected energy fluxes such as photosynthesis, which are usually not determined with conventional EC systems. The assumption of fully turbulent transport might be severely violated during stable conditions or due to the presence of significant advection arising from horizontal flow convergence/divergence or a non-zero vertically wind speed (Oncley et al., 2007). Very recently, mesoscale circulations induced by landscape-scale heterogeneity have been suggested as a potential candidate to explain the systematic underestimation of turbulent fluxes (Mauder et al., 2013; Stoy et al., 2013). Due to their low frequency, mesoscale circulations cannot be detected with a single EC station and the typical averaging time of half an hour.

EC flux data are used among others to test and calibrate land surface models (Blyth et al., 2010; Gerken et al., 2012; Gielen et al., 2010; Ingwersen et al., 2011). In these types of studies, the energy balance of EC flux data is usually post-closed, i.e. the measured turbulent fluxes are adjusted so as to force closure of the energy balance. At our current state of knowledge, however, it is unclear how to partition the missing energy. This requires modelers to make assumptions at this point, the most

BGD
11, 16911–16951, 2014

common being that the missing turbulent fluxes have the same Bowen-ratio as the measured fluxes. This method is known as the Bowen-ratio method (Barr et al., 1994; Blanken et al., 1997; Twine et al., 2000). It was applied by e.g. Blyth et al. (2010), Alavi et al. (2010), Gerken et al. (2012), Ingwersen et al. (2011), and Winter and Eltahir (2010). A second, less often applied method is to fully assign the missing energy to the latent heat flux (LE post-closure method; Falge et al., 2005; Chen et al., 2007). In a few studies, the authors decided to use the raw flux data without closing the energy balance. This decision to use a third method was made because either the authors were interested in flux patterns rather than total fluxes (Carrer et al., 2012) or they had doubts about the correctness of the Bowen-ratio method (Staudt et al., 2010). Recently, based on arguments raised by Foken (2008) and experimental findings of Mauder and Foken (2006), a fourth method has been proposed. It has been termed the sensible heat flux method (H post-closure method; Ingwersen et al., 2011) and the method fully assigns the missing energy to the sensible heat flux.

Currently, the standard approach in modeling studies is (1) to adjust the EC flux data with one post-closure (most often with the Bowen-ratio) method, (2) to indicate this post-closure method in the Material and Methods section, and (3) to evaluate model performance against the resulting data set, neglecting the possible substantial error originating from the choice of the post-closure method (Gerken et al., 2012; Alavi et al., 2010; Ingwersen et al., 2011). Only rarely has the error originating from the post-closure method been reported in the literature. Hayashi et al. (2010) used the arithmetic average of raw flux and Bowen-ratio adjusted fluxes as a measure of uncertainty. Falge et al. (2005) as well as Spank et al. (2013) plotted the difference between LE adjusted and non-adjusted flux data as a grey band to indicate the post-closure method error of the latent heat flux measurements. Our approach follows the same concept as the latter two, but our method goes further in three aspects: (1) we extend the approach for the sensible heat flux, (2) we include all three commonly used post-closure methods, and (3) we present quantitative measures to report the performance of the model with regard to the uncertainty originating from the post-closure method. We hope that this approach will help avoiding premature conclusions when models are evaluated and simulation results interpreted.

2 Material and methods

2.1 Study site and eddy covariance flux measurements

The site under study and the EC flux measurements have been described in detail elsewhere (Ingwersen et al., 2011). In brief, the study site is located in southwest Germany (48.92° N, 8.70° E). The size of the field is 425 m × 350 m. The altitude is 320 m above sea level, and the terrain is open and flat. The prevailing wind direction is south-westerly. In 2011, winter wheat (*Triticum aestivum* L. cv. Akteur) was grown. It was drilled on 11 October 2010 and harvested on 29 July 2011. Three weeks before harvest (beginning of July), the winter wheat entered the ripening phase and became progressively senescent. Soil is classified as Stagnic Luvisol (IUSS Working Group WRB, 2007). Parent material is loess with a thickness of several meters. Mean annual temperature is 9 to 10 °C, and mean annual precipitation varies between 720 and 830 mm.

From 24 March 2011 to 22 July 2011, surface energy fluxes (net radiation, sensible, latent, and soil heat flux) were measured with an EC station, which was operated in the center of the field. The station was equipped with a Licor 7500 open path infrared CO_2/H_2O gas analyzer (LI-COR Biosciences Inc., USA), CSAT3 3-D sonic anemometer (Campbell Scientific Inc., UK), NR01 4-component net radiation sensor (Hukseflux Thermal Sensors, the Netherlands), air temperature and humidity probe (HMP45C, Vaisala Inc., USA), and a tipping bucket (ARG100, Environmental Measurements LTD, UK). Close to the station, three soil heat flux plates (HFP01, Huskeflux Thermal Sensors, the Netherlands) were installed 8 cm below ground surface. Soil temperature and soil water content needed for computing the heat storage above the heat flux plate were measured with thermistor temperature probes (Model

BGD
11, 16911–16951, 2014

107, Campbell Scientific Inc., UK) installed in 2 and 6 cm and with a TDR probe (CS616, Campbell Scientific Inc. UK) installed in 5 cm depth. The EC data were processed using the software package TK3.1 (Mauder and Foken, 2011). The latent and sensible heat flux were computed from 30 min covariances between vertical wind velocity and the corresponding scalar (air humidity or air temperature). In the TK3.1 software we used the following settings: Spike detection (i.e. values exceeding 4.5 times the SD of the last 15 values were labelled as spike), planar fit method for coordinate rotation with time periods between 7 to 12 days, Moore (1986) correction except for the longitudinal separation, which was taken into account by maximizing the covariances, Schontanus et al. (1983) procedure for converting the sonic into actual temperature, and density correction as suggested by Webb et al. (1980). The version TK3.1 includes the computation of the random measurement error as the sum of instrument noise and stochastic error (Mauder et al., 2013). For data quality analysis we used the 9-flag system of Foken (1999). Half-hourly fluxes with flag 7–9 (poor quality data) for friction velocity, sensible heat flux, or latent heat flux were excluded from data analysis.

Additionally, in late autumn 2010, five subplots of 4 m^2 were randomly selected and permanently marked to track total LAI (green plus senescent LAI including stems). LAI was measured biweekly from end of March 2011 (due to the harsh winter) until crop maturity at the central square meter of every subplot using a LAI-2000 Plant Canopy Analyzer (LI-COR Biosciences Inc., USA).

2.2 Post-closure method uncertainty band

The post-closure uncertainty band (PUB) is a proxy for the possible systematic error of EC flux data due to the unknown nature of the energy balance gap. We define here that a PUB must fulfill basically two criteria: (1) the lower bound of the band must be formed by the non-adjusted measured raw fluxes, and (2) in case of EBR < 1 the width of the PUB must be non-zero for both the latent and sensible heat flux. The upper and lower bound of the band are constructed from the difference between raw fluxes

BGD
11, 16911–16951, 2014

and fluxes adjusted by one of the three post-closure methods. Figure 1 illustrates this approach for one lower and upper bound combination. The figure shows the diurnal course of simulated and measured latent and sensible heat fluxes over a winter wheat stand. The measured data were adjusted to the Bowen ratio method (line with open triangles). The difference between the Bowen ratio method and the non-adjusted fluxes (line with closed circles), the grey band between the two lines, forms the PUB. The second possible lower and upper bound combination is to use the LE and H method to construct the PUB. In the case of latent heat flux, the data adjusted with the LE method form the upper bound. In the case of the sensible heat flux, the contrary holds true. The upper bound is formed by the H adjusted data. Note that in the H method, the adjusted latent heat fluxes are identical with the raw fluxes, whereas in the LE method, the adjusted sensible heat fluxes are the same as the raw ones. The four other possible bound combinations result either in a zero PUB width for one of the two turbulent fluxes or the lower bound is not formed by the raw fluxes (Table 1). To be able to visually construct both possible PUBs, the adjusted flux that was not used in the computation of the PUB is indicated as symbols. Furthermore, to indicate the measurement error due to instrumental noise and the number of independent observations used in calculating the covariances, the random error is plotted as error bars on the measured raw fluxes.

For the construction of the PUB only half-hourly fluxes within a predefined EBR range were considered:

$$\tau < \mathrm{EBR} < 2 - \tau \tag{5}$$

Here, τ is the threshold of EBR, ranging form zero to two, that constrains the data analysis to a certain EBR window. A τ value of 0.5 means, for example, that only half-hourly fluxes with an EBR larger than 0.5 and smaller than 1.5 are considered.

Besides the above mentioned graphical representation, we suggest the following two criteria to evaluate the simulation results with respect to the PUB:

BGD
11, 16911–16951, 2014

Band coverage

The band coverage (BC) is, by definition, the percentage of simulated values that are covered by the upper and lower bound of the post-closure method uncertainty band.

Bound preference

The bound preference (BP) quantifies the average position of a simulated value within the PUB. The bound preference of the *i*th simulated value (P_i) is calculated as follows

$$BP_i = \frac{2\left(P_i - O_{LB,i}\right)}{O_{UB,i} - O_{LB,i}} - 1 \tag{6}$$

where $O_{LB,i}$ and $O_{UB,i}$ are the value of the *i*th lower and upper bound, respectively. A negative value of BP indicates that the simulated flux is closer to the lower bound, whereas a positive value indicates that the model has a preference for the upper bound. A value of zero indicates that the simulated value is midway between both bands. A BP outside the range of −1 to +1 indicates that the simulation is not enclosed by the uncertainty band. To constrain the calculation to day time values, BC and BP were computed only for mean diurnal half-hourly fluxes of sensible and latent heat larger than 20 and 40 $W m^{-2}$, respectively. The BP of the monthly mean diurnal course of a flux was computed from the median of mean half-hourly BP of that month.

2.3 The NOAH-MP land surface model

The proposed approach is demonstrated for simulations performed with the NOAH land surface model (LSM). The NOAH LSM is a well-established and widely used model. It is the land surface component of atmospheric models such as the Mesoscale Meteorology Model 5 (MM5; Dudhia, 1993), and the Weather Research and Forecasting (WRF) (e.g., Skamarock et al., 2008). Recently, the NOAH LSM has been

BGD
11, 16911–16951, 2014

extended by multiple-physics options (NOAH-MP), and an improved implementation to consider land surface heterogeneities (Niu et al., 2011). In the present study we used the version NOAH-MP v1.1 (http://www.ral.ucar.edu/research/land/technology/noahmp_lsm.php). In NOAH-MP, the land surface heterogeneity is described with a semi-tile subgrid scheme. This means that shortwave radiation transfer is computed over the entire grid cell, while longwave radiation, latent heat, sensible heat and ground heat flux are computed separately over two tiles (vegetated or bare ground area) (Niu et al., 2011). Among the many multi-physics options, the user can choose between two schemes for computing the stomatal resistance (r_s): (1) the empirical Jarvis scheme, which was already implemented in previous NOAH LSM versions, and (2) the photosynthesis-based Ball–Berry scheme. r_s is a key variable for transpiration. It strongly controls the energy partitioning at the land surface.

The Jarvis scheme computes r_s as the reciprocal product of four reduction functions, and the minimum stomatal resistance ($r_{s,\,min}$),

$$r_s = \frac{1}{\mathrm{LAI} F_1 F_2 F_3 F_4} r_{s,min} \tag{7}$$

where F_1, F_2, F_3, and F_4 are functions bounded between zero and one as lower and upper values. The four functions consider the effects of solar radiation (F_1), vapour pressure deficit (F_2), air temperature (F_3), and soil moisture stress (F_4). The variable LAI denotes the (green) leaf area index ($m^2\,m^{-2}$). For the computation of F_1 to F_4, we reference to Chen and Dudhia (2001a).

In the Ball–Berry scheme, r_s is a function of the photosynthesis rate,

$$\frac{1}{r_s} = m \frac{A}{c_{air}} \frac{e_{air}}{e_{sat}(T_v)} P_{air} + g_{min} \tag{8}$$

where A ($\mu mol\,m^{-2}\,s^{-1}$) is the rate of photosynthesis per unit LAI, c_{air} the carbon dioxide (CO_2) concentration at the leaf surface (Pa), P_{air} the surface air pressure (Pa), e_{air} the

BGD
11, 16911–16951, 2014
On the use of the post-closure method uncertainty band
J. Ingwersen et al.

vapor pressure at the leaf surface (Pa), $e_{sat}(T_v)$ the saturation vapor pressure inside the leaf (Pa), and g_{min} denotes the minimum stomatal conductance (µmol m^{-2} s^{-1}). The symbol m (1) denotes an empirical parameter that relates transpiration to CO_2 flux. A is computed with the Farquhar model (Farquhar et al., 1980) as the minimum of the enzyme ribulose bisphosphate carboxylase/oxygenase (rubisco) and light-limited rate. Moreover, a nitrogen (N) reduction factor ranging from zero to unity is included to consider N limitation. Receiving 168 kg N per hectare of fertilizer over the season the winter wheat stand on our EC site is not N limited, and the N reduction factor was set to unity.

In the following we will demonstrate the application of the PUB approach by evaluating the performance of NOAH-MP simulations to reproduce the EC flux data from a winter wheat stand and compare the performance of the Jarvis and Ball–Berry schemes. The simulation starts on day of drilling (11 October 2010) and ends on 22 July 2011 (about one week before final harvest at maturity). The soil profile was divided into four layers (0–0.1 m, 0.1–0.4 m, 0.4–1.0 m, and 1.0–2.0 m). The initial soil temperature of the four layers was 285, 283, 282, and 282 K. The initial soil water content was set to 24, 30, 41, and 43 Vol.%. We used the USGS land use dataset, vegetation type index was set to two (Dryland cropland and pasture) and soil type index was eight (silty clay loam). The multi-physics options used in the simulation are listed in Table 2. Among others, we selected a predefined monthly LAI and fractional vegetated area (FVEG) data. Monthly (green) LAI were linearly derived from measured total LAI data (Fig. 2). From mid June until mid July we assumed that the green LAI declined linearly from 4.6 to zero. FVEG was computed from the total LAI according to Nui et al. (2014) as

$$\mathrm{FVEG} = 1 - \exp(-0.52\,\mathrm{LAI}_{tot}) \quad (9)$$

The model was forced with half-hourly weather data (wind speed, air temperature, air humidity, down-welling shortwave radiation, down-welling longwave radiation, and precipitation) acquired at the EC station.

3 Results and discussion

One of the first steps in constructing the PUB is to set τ (see Eq. 5). The choice of τ is a trade-off between the average EBR, i.e. the width of the PUB, and the number of data points remaining in the dataset for model evaluation (Fig. 3). In our dataset, at $\tau = 0$ 3186 (= 100 %) half-hourly fluxes passed the quality filter, and the average EBR was 74 %. Increasing τ to 0.5 improved the EBR only slightly. At $\tau = 0.55$ both lines cross, the EBR increases to 80 %, resulting in 20 % of the fluxes which are excluded from data analysis. Increasing τ to 0.8 improves EBR considerably (to 92 %) but strongly decreases the number of data points remaining in the dataset. With this choice, 69 % of the fluxes would not be considered in model evaluation. As a consequence, the mean monthly diurnal cycle of the energy fluxes deviate markedly from that with $\tau = 0$ (Fig. 4). The diurnal cycle becomes less continuous, more scattered, and data gaps show up during the morning and evening hours. In the present study, as a compromise between the width of PUB and data loss, we set τ to 0.7. With this choice, the EBR reaches 85 %, which corresponds well with the average EBR of EC FLUXNET data (Stoy et al., 2013). The diurnal cycle of the energy fluxes is still similar to that with $\tau = 0$, and with 42 % the data loss is in an intermediate range.

Figures 5 and 6 demonstrate the standard approach to using EC flux data in model evaluation. The two figures show the diurnal course of simulated and measured latent and sensible heat flux over a winter wheat field from April to July in 2011. The simulated turbulent fluxes are compared with one data set of measured fluxes, whereby the latent and sensible heat fluxes were adjusted on the basis of one post-closure method. In this example the commonly used Bowen-ratio method was applied. With this method the modeler would come to the following interpretation: the Jarvis scheme matches nearly

BGD
11, 16911–16951, 2014

perfectly the measured latent heat fluxes in April. In May and June, however, the Jarvis scheme underestimates the observed latent heat fluxes. The agreement is less good in the morning and becomes better in the late afternoon. The tendency to underestimate the latent heat flux is even more pronounced with the Ball–Berry scheme. During the main growth period from April to June, fluxes simulated with the Ball–Berry scheme largely underestimate the latent heat flux. In July, the situation is different for both schemes. NOAH-MP also underestimates the latent heat flux in the morning, but from noon to late afternoon both schemes, which produce very similar simulation results, overestimate the latent heat flux. The above mentioned findings can be underlined by the classical performance criteria (see Table 3). The modelling efficiency (EF) of the Jarvis scheme is highest in April. The root-mean-square error (RMSE) is only 11.3 $W m^{-2}$, and the simulation is nearly unbiased. In May and June both schemes deliver negatively biased latent heat fluxes. In July, the fluxes are positively biased. Nevertheless, in all months the EF is high (78 to 99 %).

With regard to the sensible heat flux, NOAH-MP tends to overestimate the flux during the main growth period of winter wheat (Fig. 6). Simulations based on the Ball–Berry scheme largely overestimate the sensible heat flux from April to June. The bias ranges from 34.2 to 57 $W m^{-2}$, and in May the EF becomes negative (Table 3). Simulations based on the Jarvis scheme also overestimate the sensible heat flux but not as strong as those based on the Ball–Berry scheme. The EF is always higher than with the Ball–Berry scheme, and in particular in the afternoon hours of April the simulations match the measured fluxes fairly well. In July, simulations with both schemes underestimate the sensible heat flux most of the daytime (Jarvis: bias = -27.0 $W m^{-2}$; Ball–Berry: bias = -33.6 $W m^{-2}$).

In summary, the modeler would come to the conclusion that the default parameterization of NOAH-MP is not suited to simulate the surface energy fluxes at this winter wheat site. The Jarvis scheme outperformances the Ball–Berry scheme but also leads to strong systematic errors. From April to June, NOAH-MP overestimates the latent heat flux and underestimates the sensible heat flux. In July, the situation is opposite. In a next step, the modeler would try to improve the simulations, e.g. by fine-tuning of selected parameters within reasonable ranges. Ingwersen et al. (2011), for example, could distinctly improve NOAH simulations by replacing the default constant $r_{s,min}$ by fitted monthly $r_{s,min}$ values. In case of the Ball–Berry scheme an optimization of the empirical parameter m (see Eq. 7) would most probably bring the observed and simulated fluxes to a closer agreement. A further option is to search for multi-physics combinations that, with their default parameterization, lead to the best match of simulated and measured fluxes (Gayler et al., 2014).

Figures 7 to 10 show the same simulation results as above but now with the proposed PUB. First, we discuss the results based on the Bowen ratio PUB (Figs. 7 and 8). Over the daytime, the width of the PUB of the latent heat flux is on average 49.7, 59.0, 47.7, and 29.5 $\mathrm{W\,m^{-2}}$ in April, May, June, and July, respectively. The maximum width of the PUB is 88 $\mathrm{W\,m^{-2}}$ (17 % of net radiation) during noon in May. In May and June, latent heat fluxes simulated with the Jarvis scheme are well covered by the PUB (Table 4). In April, BC is only 35 %, and the Jarvis scheme has an upper bound preference (BP = 0.95, Table 4), in May and June its preference changes to the lower bound (BP = −0.29 in May and −0.49 in June). The Ball–Berry scheme has a good BC in April, and a BP of −0.53 indicates that the simulation is on average enclosed by the PUB. In May and June, the BC is poor and the BP becomes smaller than −1 pointing to a systematic underestimation of the latent heat flux though the fluxes are still in the range of the error bars. In July, the BC is low with both schemes, and in the early morning and afternoon the simulated fluxes are outside the PUB with a BP markedly larger than unity pointing to a deficiency in the model.

The mean Bowen ratios were 0.17, 0.11, and 0.12 in April, May and June, respectively, and increased over the ripening phase in July to 0.71. Because of these low Bowen ratios during the main growth period (April to June), the Bowen post-closure method assigns the majority of the energy residual to the latent heat flux, which means that the PUB of the sensible heat becomes quite narrow (Fig. 8). Most of the time both simulations do not fall within the PUB and are located above the upper bound.

BGD
11, 16911–16951, 2014

From April to June, the Ball–Berry scheme results in distinctly higher sensible heat fluxes than the Jarvis scheme. Its BP is for all three months significantly larger than unity. Particularly in May the BP reaches a value of 11.38 indicating that the simulation results are far above the upper bound of the PUB. In July, the sensible heat fluxes simulated by both schemes are only poorly matched by the PUB (BC = 5 %), but now the BP becomes negative, and the measured sensible heat fluxes are systematically underestimated from late morning to late afternoon.

As mentioned above, the Bowen ratio was low during the main growth period. Therefore, the H-LE method delivers for the latent heat flux very similar PUBs as the Bowen ratio method (Figs. 7 and 9). The width of the PUB of the LE adjusted latent heat fluxes is somewhat higher than the fluxes adjusted with the Bowen ratio method and is on average 58.3, 68.7, 56.4, and 51.0 $\mathrm{W\,m^{-2}}$ in April, May, June, and July, respectively. The maximum width of the PUB increases to 110 $\mathrm{W\,m^{-2}}$ (21 % of net radiation) and is also reached in noon in May. With regard to the sensible heat flux, in contrast, the difference between the Bowen and H-LE PUB is enormous (Figs. 8 and 10). Because the H-LE method assigns the entire energy residual to the sensible heat, the PUB becomes very broad during the daytime. The overall BC improves with either scheme (Table 5). In April, both schemes lead to a systematical overestimation of simulated sensible heat fluxes during the early morning hours. Yet, from 10 a.m. to 6 p.m., simulations with both schemes are fairly well covered by the PUB. The Jarvis scheme results in a lower bound preference (BP = −0.71), whereas the Ball–Berry scheme has an upper bound preference (BP = 0.53). In May, the simulated fluxes based on the Jarvis scheme have a BC of 100 %. The BC of the Ball–Berry scheme is 67 %. Until 2 p.m. the simulated fluxes are close to the upper bound but still within the band. After 2 p.m. the sensible heat fluxes move above the upper bound indicating a systematic overestimation during that period. In June, the BC is high with both schemes. While the fluxes simulated with the Jarvis are midway between both bands, those simulated with the Ball–Berry scheme have an upper bound preference. In July, again simulations with

BGD
11, 16911–16951, 2014

both schemes underestimate the sensible heat flux and are outside the PUB. The BP falls out of the range of −1 to 1 pointing again to a model deficiency.

The proposed PUB approach enables a more reliable interpretation of the simulation results and allows to identify more precisely periods during which the models show systematic errors. The statement, based on the evaluation on the basis of a single post-closure method, that the default parameterization of NOAH-MP is not suited to simulate the turbulent fluxes must be revised, at least for the latent heat fluxes simulated with the Jarvis scheme. It is no longer justified, because most of the time the simulations of the latent heat flux are well enclosed by the Bowen ratio and the H-LE PUB. Regarding the sensible heat flux the results are ambiguous. Based on the Bowen ratio PUB it appears that simulations with both schemes largely overestimate the sensible heat flux from April to May. According to the H-LE PUB, however, the simulated fluxes are still in the range of the uncertainty originating from the unclosed energy balance of the EC flux data. What we reliably can state is that (1) in the early morning hours of April simulations with both schemes overestimate the sensible heat flux, (2) in May the Ball–Berry scheme underestimates the latent heat flux causing that the sensible heat flux moves above the upper bound of the H-LE PUB, and (3) both schemes show a systematic error over the daytime in July.

The reason for the systematic deviation between measured and simulated sensible heat fluxes during the early morning hours in April might be related to the situation that in April the ground cover as expressed in the LAI is low. It is striking that H-LE PUB is extremely narrow during the early morning hours in April indicating a nearly perfect closure of the energy balance (Fig. 10). Due to the low ground cover in April, the illumination of the ground surface is very heterogeneous. Some positions are shaded by leaves others are sunlit. For example, while from 8 to 9 a.m. the coefficient of variation (CV) of the soil heat flux measured in 8 cm depth ($N = 3$) was 40.2 % in April, in June, due to a more homogeneous ground coverage, the CV declined to 17.9 %. Therefore, it cannot be excluded that the measured soil heat fluxes were positively

BGD
11, 16911–16951, 2014

biased. A positively biased soil heat flux reduces the available energy, results in a better closure of the energy balance, and narrows the PUB.

The systematic underestimation of the latent heat flux by Ball–Berry based simulations in May might be explained by a non-adequate parameterization of the Ball–Berry scheme in case of winter wheat. The default value of the empirical parameter m in Eq. (7), which relates transpiration to CO_2 flux, is nine as for all non-needleleaf forest USGS land use types. Mo and Liu (2001) simulated evapotranspiration (ET) and photosynthesis of winter wheat in the North China Plain and tested among others the Ball–Berry scheme. They used in their simulation for m a value of eleven. Repeating the simulation with $m = 11$ (data not shown) results in May in a nearly perfect match between simulated and measured non-adjusted latent heat fluxes (EF = 99 %), the BC of the latent heat flux increases from 4 to 41 %, the negative bias declines from −76 to $-36\,\mathrm{W\,m^{-2}}$, overall the Jarvis and Ball–Berry simulation move together, and also the simulated sensible heat fluxes are covered by the H-LE PUB.

The systematic error in July results from the fact that NOAH-MP does not distinguish between green LAI and total LAI, i.e., the sum of green living and dead senescent leaves. This makes it impossible to adequately describe the surface energy exchange from a ripening winter wheat field. In our parameterization we prescribed that the (green) LAI linearly declines from 4.6 to zero from mid June until harvest. This ensures that the transpiration, as under real field conditions, continuously decreases. In the radiation transfer scheme, however, this linearly declining LAI produces the situation that more and more shortwave radiation is absorbed by the ground instead by the vegetation. Shortly before harvest the vegetated area is treated like a bare area what is in disagreement with the real situation in the field. Also below a fully senescent winter wheat the ground is still shaded to a large fraction, because the total LAI is still high (LAI $\sim$ 3). Implementing into NOAH-MP a green LAI that is used in the stomatal resistance scheme to compute r_s and a total LAI that is applied in the radiation transfer scheme to compute the partitioning of shortwave radiation absorbed by ground and vegetation would most probably improve the simulation result in July.

BGD
11, 16911–16951, 2014

The Bowen-ratio method assumes that the Bowen-ratio is preserved over all frequency parts of the spectrum. Ruppert and Foken (2006) could show that the Bowen-ratio was not preserved for the low-frequency part of the turbulent spectra by computing the correlation coefficient of scalar similarities of water vapor and CO_2 for small and larger eddies. Wolf and Laca (2007) showed that the scalar similarity was also not given at the high-frequency edge of the turbulent spectra (frequency range between the Nyquist frequency, and the frequency at which the normalized cospectra become 10^{-3}). The high-frequency loss was more pronounced for the sensible heat flux than for the latent heat flux. While the loss for the former varied from 5 to 14 %, the latter never lost more than a few percent (2 to 5 %). Therefore, Wolf and Laca (2007) hypothesized that under their conditions underestimation of the *H* flux rather than the LE flux may explain the lack of EBC.

In the literature, a few studies compared Bowen-ratio adjusted EC fluxes against a second independent method for measuring the latent heat flux. This provides some experimental hints on the robustness of the Bowen-ratio method. Scott et al. (2010) compared ET rates obtained with the EC method against the watershed balance over a period of five years in semi-desert grassland and desert scrubland catchments in the USA. They concluded that the justification for forcing the closure using the Bowen-ratio method was ambiguous. Nine out of the investigated thirteen years showed the same or less disagreement between EC and watershed ET when measured fluxes were not adjusted. Barr et al. (2000) compared EC flux measurements with ET data obtained with the piezometric weighting lysimeter method at a boreal mature aspen stand. Over a period of 20 months, cumulative piezometric ET was 808 mm. Due to the overall low energy balance gap (on average 10 %), the two applied post-closure methods did not yield distinctly different results. Without flux adjustment, the EC method yielded a cumulative ET of 760 mm. Applying the Bowen-ratio post-closure method slightly overestimated ET but led overall to a better agreement with the lysimeter method. The Bowen-ratio post-closure method increased measured ET to 836 mm. More unambiguous results were obtained by Schume et al. (2005) and

BGD
11, 16911–16951, 2014

Wilson et al. (2001). As opposed to the two other studies described above, the EBC was distinctly lower (about 80 %). For a temperate mixed European Beech–Norway Spruce forest canopy, Schume et al. (2005) found a perfect agreement between non-adjusted latent heat flux data and the soil water balance method. Forcing the energy balance closure with the Bowen-ratio method resulted in an overestimation of ET by 16 %. For a mixed deciduous oak forest, Wilson et al. (2001) compared the EC method with the catchment water balance method. Based on the latter, the five-year average annual ET was 582 mm per year. This value agreed very well with non-adjusted ET data measured by the EC technique (571 mm $year^{-1}$). The authors did not apply any method for post-closing the energy balance, and do not give data on the Bowen-ratio, but it suffices to state that the energy balance gap correspond to about 143 mm of vaporized water. Under the climatic conditions at the site they mention (annual rainfall 1333 mm; annual ET about 580 mm), one can expect that the Bowen-ratio is distinctly lower than unity during most of the year. In other words, the Bowen-ratio method would assign most of the energy balance gap to the latent heat flux. Hence, also at the study site of Wilson et al. (2001), applying the Bowen-ratio method would have overestimated the annual ET. This short review shows that there exist experimental indications that under some conditions the Bowen-ratio method, and a fortiori the LE method, might tend to overcorrect the latent heat flux, what fits with our finding that both schemes showed a clear lower bound preference in May and June.

Studies that give experimental indications on the robustness of the *H* method are rare. Ingwersen et al. (2011) introduced the *H* method based on arguments raised by Foken (2008) and experimental findings of Mauder and Foken (2006). Foken (2008) argued that large eddies (mesoscale circulations), which cannot be captured by a single EC station and a covariance averaging time of half an hour as mentioned above, may significantly contribute to the total turbulent flux. Mauder and Foken (2006) observed that the energy residual vanished almost completely if the flux averaging time was extended from 30 min (shortwave eddies) over 24 h to 5 days (longwave eddies). The averaging time had a minor effect on the latent heat flux, but the sensible

BGD
11, 16911–16951, 2014

heat flux nearly doubled. Hence, in that data set, the energy gap could be mainly assigned to sensible heat. The approach to increase the averaging time for computing the covariance to 24 h is questionable, because it appears that this procedure violates the fundamental assumption of stationarity. The authors argue that stationarity can be still assumed, because for the investigated 16 day time series the diurnal cycle was similar each day, and the trend of adjacent averages, which is the crucial stationarity criterion for the EC method, was smaller for 24 h values than for 30 min values.

All three post-closure methods assign the energy residual to the latent and/or sensible heat flux. Such approaches assume that the available energy at the surface is measured accurately what is certainly not the case in real world. Kohsiek et al. (2007) estimated that the error in the net radiation measurement during the EBEX-2000 campaign was up to 25 $W m^{-2}$. Moreover, in the calculation of the available energy, among others, canopy storage and energy consumption by photosynthesis (gross primary productivity, GPP) are usually not considered, because they are not measured with conventional EC systems. Canopy storage becomes particularly important for tall vegetation, but can also reach 20 $W m^{-2}$ at crop sites, in particular during the morning hours (Meyers and Hollinger, 2004). On a daily average, however, this flux cancels out. Energy consumption by photosynthesis can approach fluxes in the same order of magnitude as canopy storage. For an irrigated cotton field, Oncley et al. (2007) computed for the energy consumption by photosynthesis a diurnal average value of 8 $W m^{-2}$ with a half-hourly peak value of formidable 48 $W m^{-2}$. Jacobs et al. (2008) calculated in their study all possible enthalpy changes, such as the soil heat storage, vegetation cover heat storage, dew water heat storage, air mass heat storage, and the photosynthesis energy flux for a grass land site. By doing so, they could improve the EBR of the EC flux data from 84 to 96 %. Also Leuning et al. (2012) postulated that the closure of the energy balance is possible at half-hourly time scales by careful attention to all sources of measurement and data processing errors and by accurate measurement of net radiation and every energy storage term need to calculate the available energy. Therefore, accurate measurement and considering the minor fluxes

BGD
11, 16911–16951, 2014

and storage terms in the calculation of the available energy would certainly help reducing the energy balance gap, thereby narrowing the PUB and reducing uncertainty.

The random error (instrumental noise plus stochastic error) of the EC flux measurements averaged 13 % of the latent heat flux and 11 % of the sensible heat flux. These numbers agree well with data presented by Mauder et al. (2013), who found that both errors usually range between 10 and 20 % for high-quality data as used in the present study. The instrumental noise was usually one order of magnitude lower than the stochastic error. Overall, the random error was about one order of magnitude lower than the post-closure method error, pointing to the importance of considering this error in analyzing EC flux data.

4 Conclusions

We must be aware of the fact that, by the computational adjustment of the measured fluxes, we might add a substantial bias to the observed data, no matter which post-closure method we choose. In our study the difference between the post-closing methods was up to 110 $W m^{-2}$. The possible error introduced by the post-closure method is about one order of magnitude larger than the random measurement error. This underlines the need to critically assess and communicate the possible error in eddy covariance flux data resulting from the lacking energy balance closure. The proposed post-closure method uncertainty band (PUB) approach is an effective way to achieve this. Working with only one post-closure method may result in serious misinterpretations in model-data comparisons. For narrowing the PUB, we urgently need more research on the true nature of the energy balance residual.

Acknowledgements. We gratefully acknowledge the financial support by the German Research Foundation (DFG) in the frame of the Research Unit 1695 “Agricultural Landscapes under Global Climate Change – Processes and Feedbacks on a Regional Scale”. We thank the farmers Mr. Bosch senior and Mr. Bosch junior for their cooperation.

BGD
11, 16911–16951, 2014

References

Alavi, N., Berg, A. A., Warland, J. S., Parkin, G., Verseghy, D., and Bartlett, P.: Evaluating the impact of assimilating soil moisture variability data on latent heat flux estimation in a land surface model, Can. Water Resour. J., 35, 157–172, 2010.

Baldocchi, D., Reichstein, M., Papale, D., Koteen, L., Vargas, R., Agarwal, D., and Cook, R.: The role of trace gas flux networks in the biogeosciences, Eos T. Am. Geophys. Un., 93, 217–218, 2012.

Barr, A. G., King, K. M., Gillespie, T. J., den Hartog, G., and Neumann, H. H.: A comparison of Bowen ratio and eddy correlation sensible and latent heat flux measurements above deciduous forest, Bound.-Lay. Meteorol., 71, 21–41, 1994.

Barr, A. G., Kamp, G. V. D., Schmidt, R., and Black, T. A.: Monitoring the moisture balance of a boreal aspen forest using a deep groundwater piezometer, Agr. Forest Meteorol., 102, 13–24, 2000.

Blanken, P. D., Black, T. A., Yang, P. C., Neumann, H. H., Nesic, Z., Staebler, R., Den Hartog, G., Novak, M. D., and Lee, X.: Energy balance and canopy conductance of a boreal aspen forest: partitioning overstory and understory components, J. Geophys. Res.-Atmos., 102, 28915–28927, 1997.

Blyth, E., Gash, J., Lloyd, A., Pryor, M., Weedon, G. P., and Shuttleworth, J.: Evaluating the JULES land surface model energy fluxes using FLUXNET data, J. Hydrometeorol., 11, 509–519, 2010.

Carrer, D., Lafont, S., Roujean, J.-L., Calvet, J.-C., Meurey, C., Le Moigne, P., and Trigo, I. F.: Incoming solar and infrared radiation derived from METEOSAT: impact on the modeled land water and energy budget over France, J. Hydrometeorol., 13, 504–520, 2012.

Chen, F. F. and Dudhia, J.: Coupling and advanced land surface-hydrology model with the Penn State-NCAR MM5 modeling system. Part I: Model implementation and sensitivity, Mon. Weather Rev., 129, 569–585, 2001.

Chen, F. F., Manning, K. W., Lemone, M. A., Trier, S. B., Alfieri, J. G., Roberts, R., Tewari, M., Niyogi, D., Horst, T. W., Oncley, S. P., Basara, J. B., and Blanken, P. D.: Description and evaluation of the characteristics of the NCAR high-resolution land data assimilation system, J. Appl. Meteorol. Clim., 46, 694–713, 2007.

Dudhia, J.: A nonhydrostatic version of the Penn State-NCAR mesoscale model: validation tests and simulation of an Atlantic cyclone and cold front, Mon. Weather Rev., 121, 1493–1513, 1993.
Falge, E., Reth, S., Brüggemann, N., Butterbach-Bahl, K., Goldberg, V., Oltchev, A., Schaaf, S., Spindler, G., Stiller, B., Queck, R., Köstner, B., and Bernhofer, C.: Comparison of surface energy exchange models with eddy flux data in forest and grassland ecosystems of Germany, Ecol. Model., 188, 174–216, 2005.
Farquhar, G. D., von Caemmerer, S., and Berry, J. A.: A biochemical model of photosynthetic CO_2 assimilation in leaves of C_3 species, Planta, 149, 78–90, 1980.
Foken, T. T.: Der Bayreuther Turbulenzknecht, Universität Bayreuth, 1999 (in German).
Gayler, S., Wöhling, T., Grzeschik, M., Ingwersen, J., Wizemann, H.-D., Warrach-Sagi, K., Högy, P., Attinger, S., Streck, T., and Wulfmeyer, V.: Incorporating dynamic root growth enhances the performance of Noah-MP at two contrasting winter wheat field sites, Water Resour. Res., 50, 1337–1356, 2014.
Gerken, T., Babel, W., Hoffmann, A., Biermann, T., Herzog, M., Friend, A. D., Li, M., Ma, Y., Foken, T., and Graf, H.-F.: Turbulent flux modelling with a simple 2-layer soil model and extrapolated surface temperature applied at Nam Co Lake basin on the Tibetan Plateau, Hydrol. Earth Syst. Sci., 16, 1095–1110, doi:10.5194/hess-16-1095-2012, 2012.
Gielen, B., Verbeeck, H., Neirynck, J., Sampson, D. A., Vermeiren, F., and Janssens, I. A.: Decadal water balance of a temperate Scots pine forest (*Pinus sylvestris* L.) based on measurements and modelling, Biogeosciences, 7, 1247–1261, doi:10.5194/bg-7-1247-2010, 2010.
Hayashi, M., Jackson, J. F., and Xu, L.: Application of the versatile soil moisture budget model to estimate evaporation from prairie grassland, Can. Water Resour. J., 35, 187–208, 2010.
Ingwersen, J., Steffens, K., Högy, P., Warrach-Sagi, K., Zhunusbayeva, D., Poltoradnev, M., Gäbler, R., Wizemann, H.-D., Fangmeier, A., Wulfmeyer, V., and Streck, T.: Comparison of Noah simulations with eddy covariance and soil water measurements at a winter wheat stand, Agr. Forest Meteorol., 151, 345–355, 2011.
IUSS Working Group WRB: World Reference Base for Soil Resources 2006, first update 2007, Rome, FAO, 2007.
Jacobs, A. F. G., Heusinkveld, B. G., and Holtslag, A. A. M.: Towards closing the surface energy budget of a mid-latitude grassland, Bound.-Lay. Meteorol., 126, 125–136, 2008.

BGD
11, 16911–16951, 2014

On the use of the post-closure method uncertainty band

J. Ingwersen et al.

Kohsiek, W., Liebethal, C., Foken, T., Vogt, R., Oncley, S. P., Bernhofer, C., and Debruin, H. A. R.: The Energy Balance Experiment EBEX-2000. Part III: Behaviour and quality of the radiation measurements, Bound.-Lay. Meteorol., 123, 55–75, 2007.
Leuning, R., van Gorsel, E., Massman, W. J., and Isaac, P. R.: Reflections on the surface energy imbalance problem, Agr. Forest Meteorol., 156, 65–74, 2012.
LI-COR Inc.: EddyPro, available at: www.licor.com/eddypro, 2012.
Mauder, M. and Foken, T.: Documentation and Instruction Manual of the Eddy-Covariance Software Package TK3, Universität Bayreuth, Abteilung Mikrometeorologie, 2011.
Mauder, M., Cuntz, M., Drüe, C., Graf, A., Rebmann, C., Schmid, H. P., Schmidt, M., and Steinbrecher, R.: A strategy for quality and uncertainty assessment of long-term eddy-covariance measurements, Agr. Forest Meteorol., 169, 122–135, 2013.
Mauder, M. M. and Foken, T. T.: Impact of post-field data processing on eddy covariance flux estimates and energy balance closure, Meteorol. Z., 15, 597–609, 2006.
Meyers, T. P. and Hollinger, S. E.: An assessment of storage terms in the surface energy balance of maize and soybean, Agr. Forest Meteorol., 125, 105–115, 2004.
Mo, X. and Liu, S.: Simulating evapotranspiration and photosynthesis of winter wheat over the growing season, Agr. Forest Meteorol., 109, 203–222, 2001.
Moore, C. J.: Frequency response corrections for eddy correlation systems, Bound.-Lay. Meteorol., 37, 17–35, 1986.
Niu, G.-Y. Yang, Z.-L., Mitchell, K. E., Chen, F., Ek, M. B., Barlage, M., Kumar, A., Manning, K., Niyogi, D., Rosero, E., Tewari, M., and Xia, Y.: The community Noah land surface model with multiparameterization options (Noah-MP): 1. Model description and evaluation with local-scale measurements, J. Geophys. Res.-Atmos., 116, D12109, doi:10.1029/2010JD015139, 2011.
Oncley, S. P., Foken, T., Vogt, R., Kohsiek, W., DeBruin, H. A. R., Bernhofer, C., Christen, A., van Gorsel, E., Grantz, D., Feigenwinter, C., Lehner, I., Liebethal, C., Liu, H., Mauder, M., Pitacco, A., Ribeiro, L., and Weidinger, T.: The energy balance experiment EBEX-2000. Part I: Overview and energy balance, Bound.-Lay. Meteorol., 123, 1–28, 2007.
Ruppert, J. J., Thomas, C., and Foken, T. T.: Scalar similarity for relaxed eddy accumulation methods, Bound.-Lay. Meteorol., 120, 39–63, 2006.
Schotanus, P., Nieuwstadt, F. T. M., and DeBruin, H. A. R.: Temperature measurement with a sonic anemometer and its application to heat and moisture fluctuations, Bound.-Lay. Meteorol., 26, 81–93, 1983.

BGD
11, 16911–16951, 2014

Schume, H., Hager, H., and Jost, G.: Water and energy exchange above a mixed European Beech – Norway Spruce forest canopy: a comparison of eddy covariance against soil water depletion measurement, Theor. Appl. Climatol., 81, 87–100, 2005.
Scott, R. L. R. L.: Using watershed water balance to evaluate the accuracy of eddy covariance evaporation measurements for three semiarid ecosystems, Agr. Forest Meteorol., 150, 219–225, 2010.
Skamarock, W. C., Klemp, J. B., Dudhia, J., Gill, D. O., Barker, D. M., Duda, M. G., Huang, X. Y., Wang, W., and Powers, J. G.: A description of the Advanced Research WRF Version 3, NCAR Technical Note, 2008.
Spank, U., Schwärzel, K., Renner, M., Moderow, U., and Bernhofer, C.: Effects of measurement uncertainties of meteorological data on estimates of site water balance components, J. Hydrol., 492, 176–189, 2013.
Staudt, K., Falge, E., Pyles, R. D., Paw U, K. T., and Foken, T.: Sensitivity and predictive uncertainty of the ACASA model at a spruce forest site, Biogeosciences, 7, 3685–3705, doi:10.5194/bg-7-3685-2010, 2010.
Stoy, P. C., Mauder, M., Foken, T., Marcolla, B., Boegh, E., Ibrom, A., Arain, M. A., Arneth, A., Aurela, M., Bernhofer, C., Cescatti, A., Dellwik, E., Duce, P., Gianelle, D., van Gorsel, E., Kiely, G., Knohl, A., Margolis, H., Mccaughey, H., Merbold, L., Montagnani, L., Papale, D., Reichstein, M., Saunders, M., Serrano-Ortiz, P., Sottocornola, M., Spano, D., Vaccari, F., and Varlagin, A.: A data-driven analysis of energy balance closure across FLUXNET research sites: the role of landscape scale heterogeneity, Agr. Forest Meteorol., 171–172, 137–152, 2013.
Twine, T. E., Kustas, W. P., Norman, J. M., Cook, D. R., Houser, P. R., Meyers, T. P., Prueger, J. H., Starks, P. J., and Wesely, M. L.: Correcting eddy-covariance flux underestimates over a grassland, Agr. Forest Meteorol., 103, 279–300, 2000.
Webb, E. K., Pearman, G. I., and Leuning, R.: Correction of the flux measurements for density effects due to heat and water vapour transfer, Q. J. Roy. Meteor. Soc., 106, 85–100, 1980.
Wilson, K. K., Goldstein, A., Falge, E., Aubinet, M., Baldocchi, D., Berbigier, P., Bernhofer, C., Ceulemans, R., Dolman, H., Field, C., Grelle, A., Ibrom, A., Law, B. E., Kowalski, A., Meyers, T., Moncrieff, J., Monson, R., Oechel, W., Tenhunen, J., Valentini, R., and Verma, S.: Energy balance closure at FLUXNET sites, Agr. Forest Meteorol., 113, 223–243, 2002.
Wilson, K. B., Hanson, P. J., Mulholland, P. J., Baldocchi, D. D., and Wullschleger, S. D.: A comparison of methods for determining forest evapotranspiration and its components: sap-

flow, soil water budget, eddy covariance and catchment water balance, Agr. Forest Meteorol., 106, 153–168, 2001.
Winter, J. M. and Eltahir, E. A. B.: The sensitivity of latent heat flux to changes in the radiative forcing: a framework for comparing models and observations, J. Climate, 23, 2345–2356, 2010.
Wolf, A. and Laca, E. A.: Cospectral analysis of high frequency signal loss in eddy covariance measurements, Atmos. Chem. Phys. Discuss., 7, 13151–13173, doi:10.5194/acpd-7-13151-2007, 2007.

BGD
11, 16911–16951, 2014
On the use of the post-closure method uncertainty band
J. Ingwersen et al.

Table 1. Overview of possible bound combinations to construct the post-closure method uncertainty band (PUB). The upper and lower bound of the band are constructed from the difference between raw fluxes and fluxes adjusted by one of the three post-closure methods (Bowen ratio (B), sensible heat (H), and latent heat (LE) method).

Bound combination	Lower bound = measured flux		PUB width > 0		Useful combination
	LE	H	LE	H	
1. H-LE	y	y	y	y	**y**
2. H-B	y	n	y	y	n
3. LE-B	n	y	y	y	n
4. raw-LE	y	y	y	n	n
5. raw-H	y	y	n	y	n
6. raw-B	y	y	y	y	**y**

y: yes; n: no.

BGD
11, 16911–16951, 2014

J. Ingwersen et al.

Table 2. Setting of the multi-physics options used in the NOAH-MP simulation.

Multi-physics option	Setting
Vegetation model	opt_dveg = 1: LAI and FVEG pre-defined in look-up table
Canopy stomatal resistance scheme	opt_crs = 1 or 2: Ball–Berry (1) or Jarvis (2) scheme
Runoff and groundwater model	opt_btr = 1: TOPMODEL-based simple groundwater model
Sensible heat exchange coefficient	opt_sfc = 1: Based on Monin–Obukov similarity theory
Super-cooled liquid water	opt_frz = 1: General form of the of the freezing-point depression equation (NY06)
Radiation transfer scheme	opt_rad = 3: Gaps = 1-FVEG
Lower boundary of soil temperature	opt_tbot = 2: Constant temperature
Snow/soil temperature time scheme	opt_stc = 1: Semi-implicit

LAI: (green) leaf area index; FVEG: fractional vegetated area.

Discussion Paper | Discussion Paper | Discussion Paper | Discussion Paper |

BGD

11, 16911–16951, 2014

On the use of the post-closure method uncertainty band

J. Ingwersen et al.

Title Page
Abstract Introduction
Conclusions References
Tables Figures
◀◀ ▶▶
◀ ▶
Back Close
Full Screen / Esc

Printer-friendly Version

Interactive Discussion

Table 3. Model performance criteria for the simulation results presented in Figs. 4 and 5. For the computation of model efficiency, root mean square error (RMSE) and bias see, for example, Ingwersen et al. (2011). The performance criteria were computed for the daytime (6 a.m. to 6 p.m.).

Month	Model efficiency (%)		RMSE ($W m^{-2}$)		Bias ($W m^{-2}$)	
	Jarvis	Ball–Berry	Jarvis	Ball–Berry	Jarvis	Ball–Berry
Latent heat flux						
Apr	99	93	11.3	35.7	1.0	−26.4
May	96	83	40.9	81.4	−36.3	−76.0
Jun	95	91	41.1	52.2	−39.7	−51.1
Jul	84	78	34.1	39.1	7.4	18.3
Sensible heat flux						
Apr	91	59	16.8	36.2	8.9	34.2
May	78	−45	23.3	60.2	22.5	57.0
Jun	69	36	26.9	38.4	25.4	36.6
Jul	92	89	38.9	45.2	−27.0	−33.6

BGD
11, 16911–16951, 2014

Table 4. Evaluation criteria of the Bowen ratio post-closure method uncertainty bands presented in Figs. 7 and 8.

Month	Band coverage (%)		Bound preference (1)	
	Jarvis	Ball–Berry	Jarvis	Ball–Berry
Latent heat flux				
Apr	35	70	0.95	−0.53
May	74	4	−0.29	−1.67
Jun	67	33	−0.49	−1.15
Jul	7	7	1.96	2.67
Sensible heat flux				
Apr	31	0	1.48	6.87
May	0	0	4.77	11.38
Jun	0	0	6.37	8.31
Jul	5	5	−2.26	−2.81

BGD
11, 16911–16951, 2014

Table 5. Evaluation criteria of the post-closure method uncertainty bands (PUB) presented in Figs. 9 and 10. The PUB was computed from the difference between sensible heat (H) and latent heat (LE) adjusted fluxes.

Month	Band coverage (%)		Bound preference (1)	
	Jarvis	Ball–Berry	Jarvis	Ball–Berry
Latent heat flux				
Apr	52	70	0.58	−0.57
May	70	4	−0.35	−1.60
Jun	71	36	−0.57	−1.09
Jul	26	26	1.22	1.77
Sensible heat flux				
Apr	76	76	−0.71	0.53
May	100	67	−0.15	0.80
Jun	100	100	0.07	0.40
Jul	18	14	−1.57	−1.73

BGD
11, 16911–16951, 2014

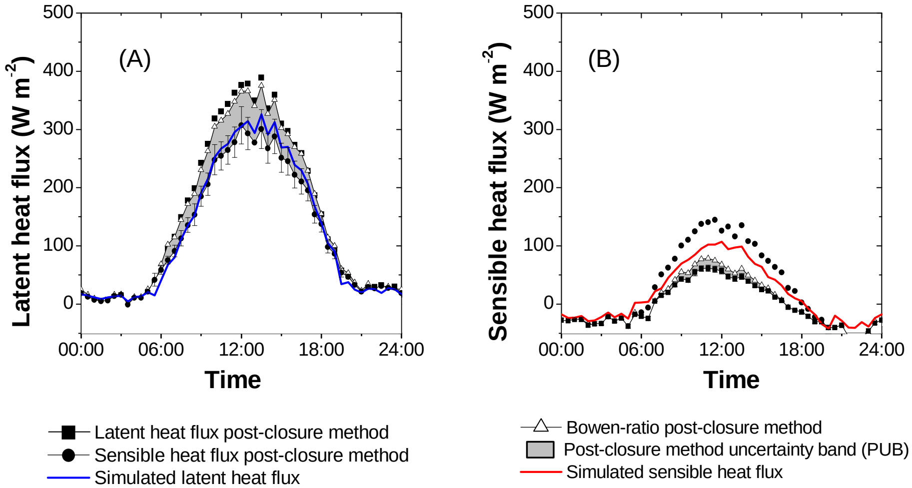

Figure 1. Illustration of the post-closure method uncertainty band (PUB) to consider the systematic error in eddy covariance (EC) flux data. The grey band shows the PUB computed as the difference between Bowen-ratio adjusted and non-adjusted fluxes. The closed squares in **(a)** indicate the latent heat (LE) post-closed fluxes, and the closed circles in **(b)** show the sensible heat (H) post-closed data. Note: in case of latent heat flux, raw data and H post-closed data are identical. In case of sensible heat flux, LE post-closed data and raw data are identical.

BGD
11, 16911–16951, 2014

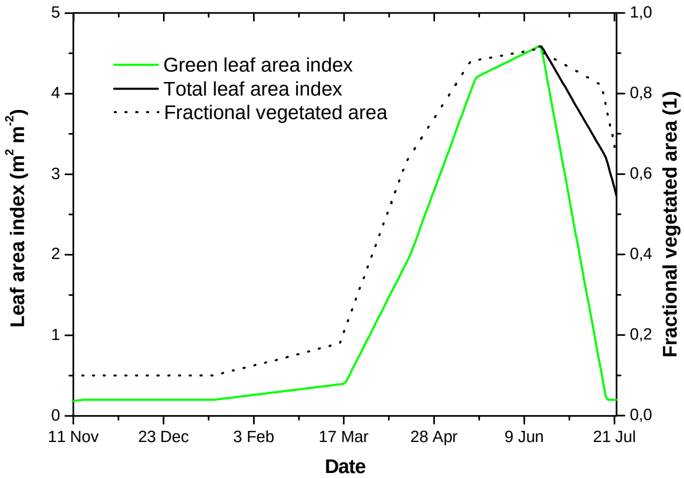

Figure 2. Prescribed dynamics of the green and total leaf area index and the fractional vegetated area used in NOAH-MP simulations. Note: until 15 June green and total leaf area index are the same.

BGD
11, 16911–16951, 2014

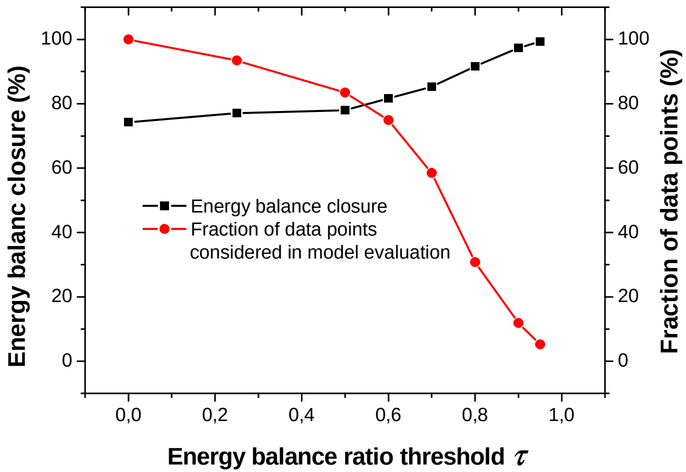

Figure 3. Effect of the energy balance ratio threshold τ on the energy balance closure and the fraction of data points remaining in the dataset for model evaluation.

BGD
11, 16911–16951, 2014

On the use of the post-closure method uncertainty band

J. Ingwersen et al.

Title Page
Abstract | Introduction
Conclusions | References
Tables | Figures
◀| |▶
◀ ▶
Back | Close
Full Screen / Esc
Printer-friendly Version
Interactive Discussion

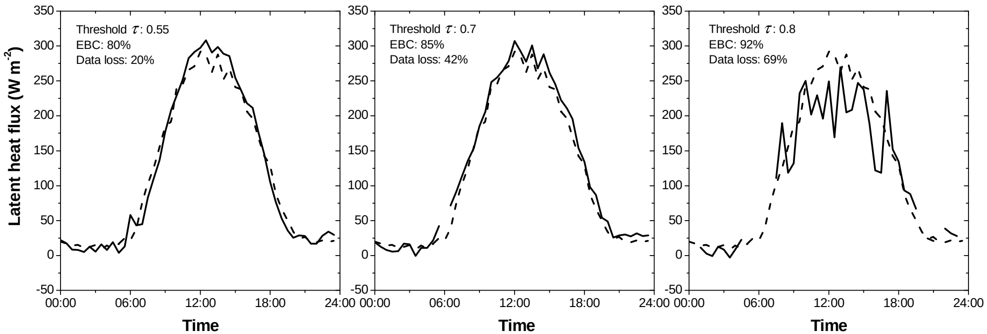

Figure 4. Effect of the energy balance ratio threshold τ on the pattern of the mean diurnal cycle of measured latent heat fluxes in May 2011. The dotted line shows the mean diurnal course for τ = zero, i.e. only flux data with an energy balance ratio (EBR) $\tau < \text{EBR} < 2-\tau$ were used to compute the mean diurnal course.

BGD
11, 16911–16951, 2014

Title Page
Abstract | Introduction
Conclusions | References
Tables | Figures
◀I | ▶I
◀ | ▶
Back | Close
Full Screen / Esc
Printer-friendly Version
Interactive Discussion

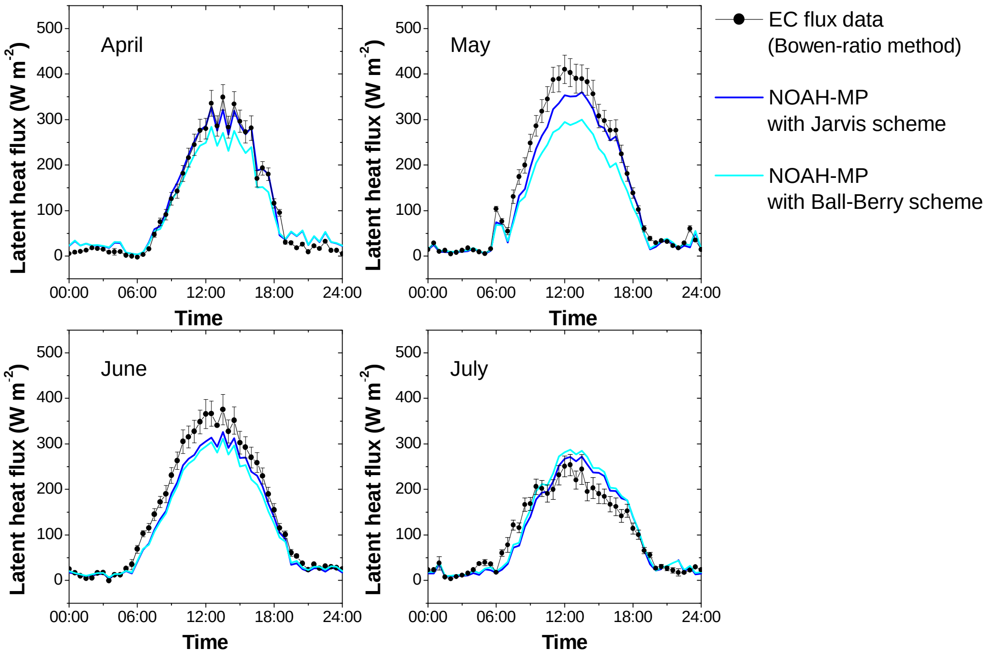

Figure 5. State-of-the art approach to compare simulated and measured eddy covariance (EC) flux data. The monthly average diurnal cycles of latent heat flux were computed based on Bowen-ratio post-closed data. For modeling the NOAH-MP land surface model was used in two configurations. The stomatal resistance was computed either with the empirical Jarvis scheme or the photosynthesis-based Ball–Berry scheme. The simulated fluxes are compared with measured EC flux data that were adjusted with the Bowen-ratio method.

BGD
11, 16911–16951, 2014

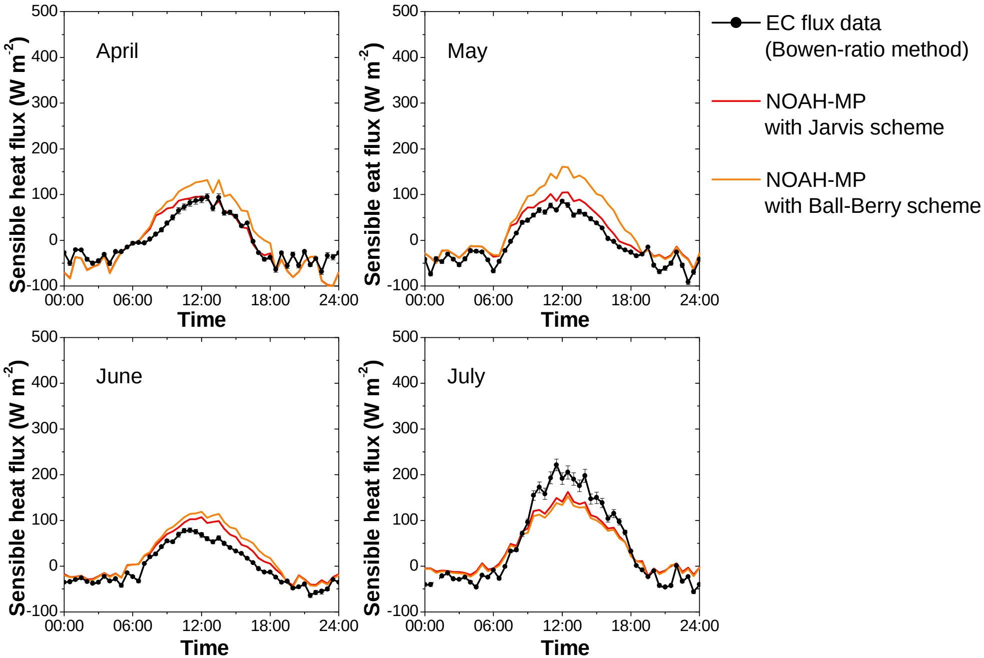

Figure 6. State-of-the art approach to compare simulated and measured eddy covariance flux data. The monthly average diurnal cycles of sensible heat flux were computed based on Bowen-ratio post-closed data. For modeling the NOAH-MP land surface model was used in two configurations. The stomatal resistance was computed either with the empirical Jarvis scheme or the photosynthesis-based Ball–Berry scheme. The simulated fluxes are compared with measured eddy covariance (EC) flux data that were adjusted with the Bowen-ratio method.

BGD
11, 16911–16951, 2014

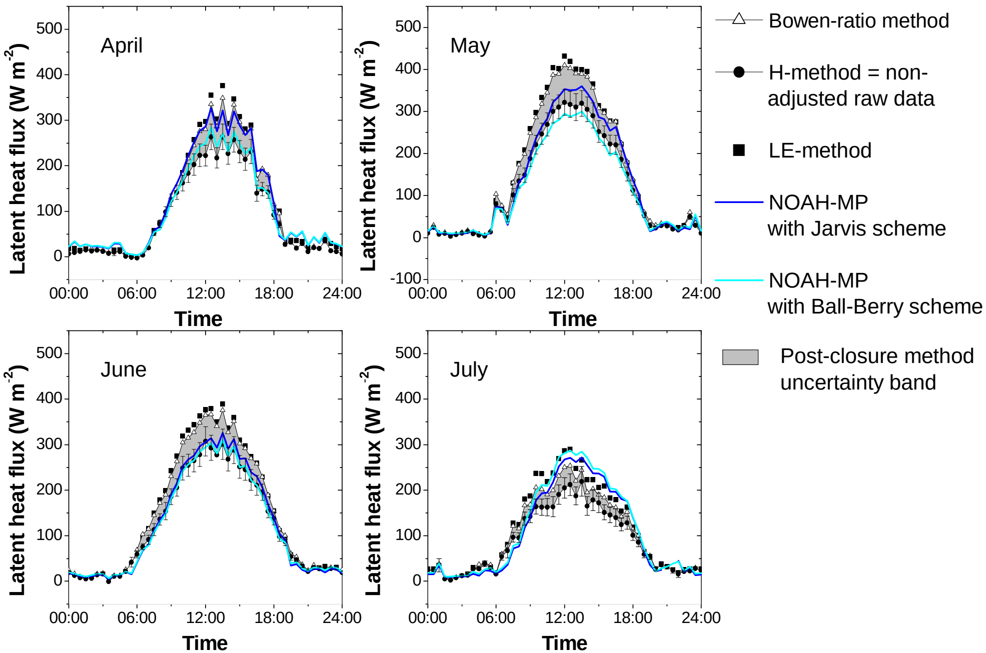

Figure 7. Measured and simulated monthly average diurnal cycles of latent heat flux over a winter wheat stand in southwest Germany. For modeling the NOAH-MP land surface model was used in two configurations. The stomatal resistance was computed either with the empirical Jarvis scheme or the photosynthesis-based Ball–Berry scheme. The grey band shows the post-closure method uncertainty band computed as the difference between the raw and Bowen-ratio adjusted fluxes. The error bars indicate the random error (instrumental noise plus stochastic error) of the eddy covariance (EC) measurement.

BGD
11, 16911–16951, 2014

On the use of the post-closure method uncertainty band

J. Ingwersen et al.

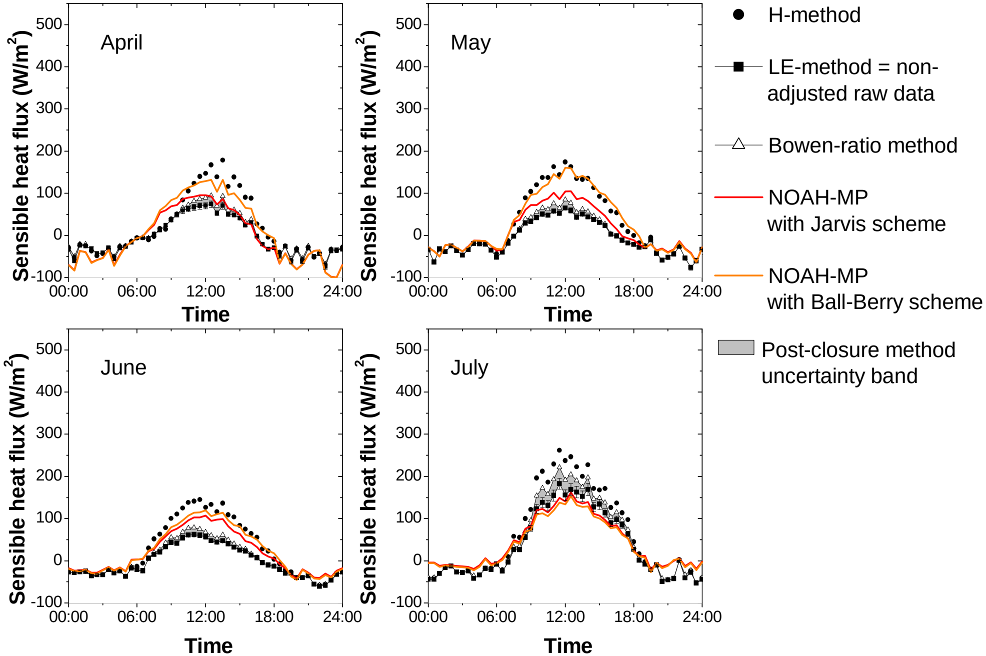

Figure 8. Measured and simulated monthly average diurnal cycles of sensible heat flux over a winter wheat stand in southwest Germany. For modeling the NOAH-MP land surface model was used in two configurations. The stomatal resistance was computed either with the empirical Jarvis scheme or the photosynthesis-based Ball–Berry scheme. The grey band shows the post-closure method uncertainty band computed as the difference between the raw and Bowen-ratio adjusted fluxes. The error bars indicate the random error (instrumental noise plus stochastic error) of the eddy covariance (EC) measurement.

BGD
11, 16911–16951, 2014

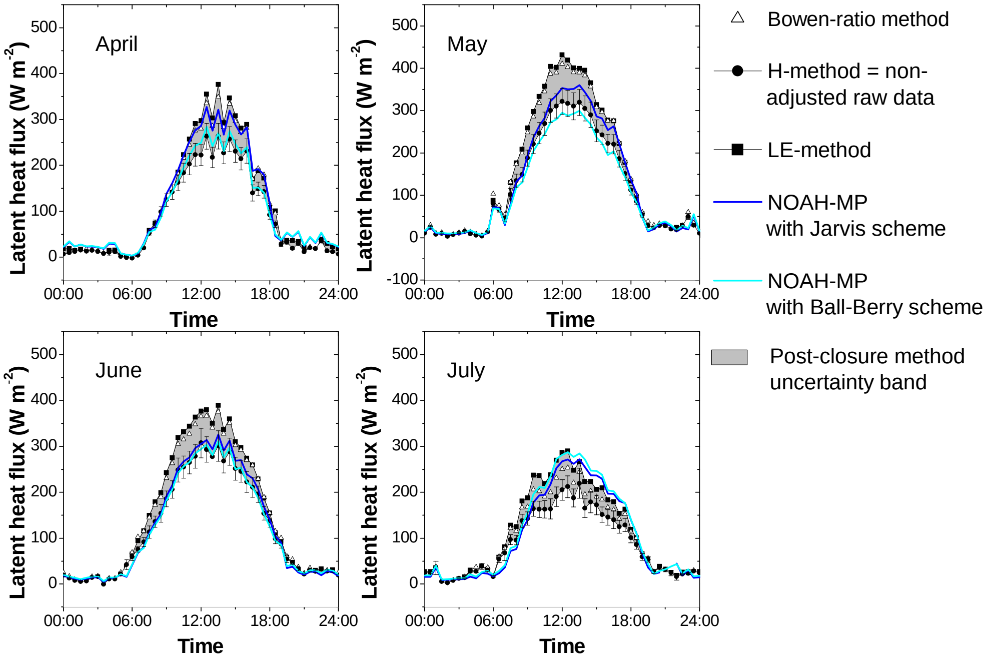

Figure 9. Measured and simulated monthly average diurnal cycles of latent heat flux over a winter wheat stand in southwest Germany. For modeling the NOAH-MP land surface model was used in two configurations. The stomatal resistance was computed either with the empirical Jarvis scheme or the photosynthesis-based Ball–Berry scheme. The grey band shows the post-closure method uncertainty band (PUB) computed as the difference between sensible heat (H) and latent heat (LE) adjusted fluxes. The error bars indicate the random error (instrumental noise plus stochastic error) of the eddy covariance (EC) measurement.

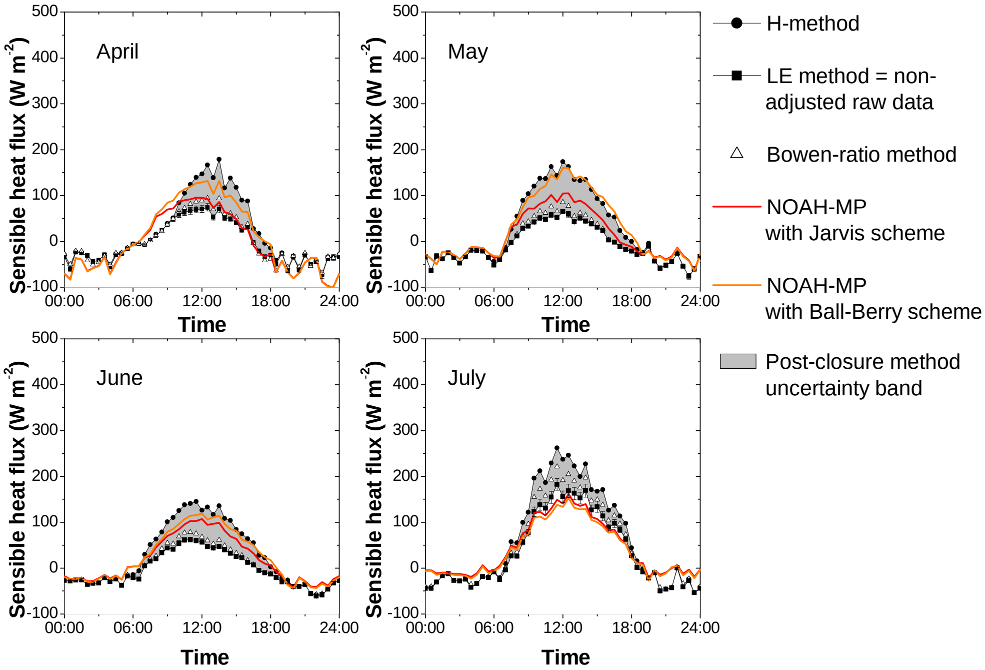

Figure 10. Measured and simulated monthly average diurnal cycles of sensible heat flux over a winter wheat stand in southwest Germany. For modeling the NOAH-MP land surface model was used in two configurations. The stomatal resistance was computed either with the empirical Jarvis scheme or the photosynthesis-based Ball–Berry scheme. The grey band shows the post-closure method uncertainty band (PUB) computed as the difference between sensible heat (*H*) and latent heat (LE) adjusted fluxes. The error bars indicate the random error (instrumental noise plus stochastic error) of the eddy covariance (EC) measurement.

BGD
11, 16911–16951, 2014

On the use of the post-closure method uncertainty band

J. Ingwersen et al.